

Three-Dimensional Genus Statistics of Galaxies in the SDSS Early Data Release

Chiaki HIKAGE¹, Yasushi SUTO,¹ Issha KAYO¹, Atsushi TARUYA¹,

Takahiko MATSUBARA², Michael S. VOGLEY³, Fiona HOYLE³,

J. Richard GOTT III⁴, Jon BRINKMANN⁵, for the SDSS collaboration

¹*Department of Physics, School of Science, University of Tokyo, Tokyo 113-0033*

²*Department of Physics and Astrophysics, Nagoya University, Chikusa, Nagoya 161-8602*

³*Department of Physics, Drexel University, 3141 Chestnut Street, Philadelphia, PA 19104, USA*

⁴*Princeton University Observatory, Peyton Hall, Princeton, NJ 08544, USA*

⁵*Apache Point Observatory, P.O.Box 59, Sunspot NM 88349-0059, USA*

hikage@utap.phys.s.u-tokyo.ac.jp, suto@phys.s.u-tokyo.ac.jp, kayo@utap.phys.s.u-tokyo.ac.jp,

ataruya@utap.phys.s.u-tokyo.ac.jp, taka@a.phys.nagoya-u.ac.jp,

hoyle@venus.physics.drexel.edu, vogley@drexel.edu, jrg@astro.princeton.edu, jb@apo.nmsu.edu

(Received 2002 July 18; accepted 2002)

Abstract

We present the first analysis of three-dimensional genus statistics for the SDSS EDR galaxy sample. Due to the complicated survey volume and the selection function, analytic predictions of the genus statistics for this sample are not feasible, therefore we construct extensive mock catalogs from N-body simulations in order to compare the observed data with model predictions. This comparison allows us to evaluate the effects of a variety of observational systematics on the estimated genus for the SDSS sample, including the shape of the survey volume, the redshift distortion effect, and the radial selection function due to the magnitude limit. The observed genus for the SDSS EDR galaxy sample is consistent with that predicted by simulations of a Λ -dominated spatially-flat cold dark matter model. Standard ($\Omega_0 = 1$) cold dark matter model predictions do not match the observations. We discuss how future SDSS galaxy samples will yield improved estimates of the genus.

Key words: cosmology: large-scale structure of universe — cosmology: observations — galaxies: distances and redshifts — methods: statistical

1. Introduction

Characterizing the large-scale distribution of galaxies and clusters is critical for understanding the formation and evolution of this structure as well as for probing the initial conditions of the universe itself. The most widely used statistical measure for this purpose is the two-point correlation function (2PCF). This statistic is easily estimated, is simply parametrized, and is well-studied. The observed correlation function is approximately a power law over a finite range of scales (Totsuji & Kihara 1969), and thus can be expressed by two numbers, the power-law slope and the correlation length. This correlation function statistic has been successfully applied in the cosmological context for more than 30 years, thus its behavior is well understood theoretically. Given a set of cosmological parameters, one can predict the corresponding mass 2PCF $\xi(r, z)$ on a scale r at a redshift z using accurate fitting formulae (e.g., Hamilton et al. 1991; Peacock & Dodds 1996). In principle, the spatial biasing of luminous objects relative to the underlying dark matter may invalidate the straightforward comparison between observations and theoretical predictions. However, the SDSS galaxy sample which we analyze is consistent with a (practically) scale-independent linear bias on scales of $(0.2 - 4)h^{-1}\text{Mpc}$ if one adopts the currently popular Λ -dominated spatially-flat cold dark matter (LCDM) model (Kayo et al. 2002).

While the 2PCF and its Fourier transform the power spectrum are the most convenient and useful cosmological statistics, they completely ignore information about the correlations of the phases of the density fluctuations in k -space. In contrast, the topology of large-scale structure, as measured by the genus statistic (Gott, Melott, & Dickinson 1986) is strongly sensitive to these phase correlations. One of the Minkowski functionals (Mecke, Buchert & Wagner 1994; Schmalzing & Buchert 1997) is closely related to the genus. Other statistics that quantify phase correlations in the data include higher-order n -point correlation functions (e.g., Peebles 1980 and references therein), percolation analysis (Shandarin 1983), minimal spanning trees (Barrow, Bhavsar & Sonoda 1985), and void statistics (White 1979). We focus on the genus mainly because its behavior is well-understood theoretically; if the primordial fluctuations are Gaussian, then the genus in the linear regime has an exact analytic expression (see eq. [4] below). The theoretical prediction for a Gaussian random field makes it clear that only the amplitude of the genus depends on the 2PCF, while higher order correlations determine the shape as well as affecting the amplitude. Thus, the shape of the genus statistic plays a complementary role to the 2PCF. In addition to the linear theory predictions, a perturbative expression for the genus in the weakly nonlinear regime has been obtained by Matsubara (1994) and the log-normal model is shown to be a good empirical approximation in the strongly nonlinear regime (e.g., Coles & Jones 1991; Hikage, Taruya & Suto 2002).

Previous to the SDSS, investigations of the the 3D genus statistic for galaxy redshift surveys include Gott et al. (1989), Park, Gott & da Costa (1992), Moore et al. (1992) Rhoads

et al. (1994), Vogeley et al. (1994), and Canavezes et al. (1998). As suggested by Melott (1987), the 2D variant of this statistic has been estimated for a variety of data sets by Coles & Plionis (1991), Plionis, Valdarnini & Coles (1992), Park et al. (1992), Colley (1997), Park, Gott, & Choi (2001), and Hoyle, Vogeley & Gott (2002a). These investigations generally indicate consistency with the hypothesis that the initial perturbations were Gaussian in nature. Some departures from Gaussianity have been suggested, but the statistical significance of the results was low due to the small size of the available data sets. Hoyle et al. (2002b) find weak evidence for variation in the genus with galaxy type in the SDSS using the 2D genus statistic.

In the present paper, we describe the first analysis of the 3D genus of the SDSS early data release galaxy sample. We evaluate a variety of observational effects using mock catalogs from N-body simulations such as the shape of the survey volume, the redshift distortion effect, and the radial selection function due to the magnitude limit. To within the uncertainties for this preliminary sample, we find that the LCDM model reasonably reproduces the observed shape and amplitude of the genus of SDSS galaxies. A complementary analysis of the 2D genus for the SDSS galaxies is presented separately in Hoyle et al. (2002b). Other analyses of early SDSS data include measurement of the power spectrum (Szalay et al. 2002; Tegmark et al. 2002; Dodelson et al. 2002), correlation function (Zehavi et al. 2002; Connolly et al. 2002; Infante et al. 2002), and higher-order moments (Szapudi et al. 2002).

The outline of the paper is as follows. In section 2 we describe the SDSS Early Data Release sample that we analyze. To analyze systematic effects we use mock samples drawn from N-body simulations, which are described in section 3. Section 4 describes the genus statistic and the method of estimation. Observational systematics are analyzed in section 5. Genus results for the SDSS EDR sample are presented in section 6. Section 7 presents our conclusions.

2. SDSS galaxy data

The early data release sample of the SDSS includes five-color CCD imaging and moderate-resolution spectroscopy of galaxies in Northern and Southern equatorial stripes of width 2.5° in declination and in another stripe that overlaps the SIRTf First Look Survey. York et al. (2000) provide an overview of the SDSS. Stoughton et al. (2002) describe the early data release (EDR) and details about the measurements. Technical articles providing details of the SDSS include description of the photometric camera (Gunn et al. 1998), photometric analysis (Lupton et al. 2002), the photometric system (Fukugita et al. 1996; Hogg et al. 2001; Smith et al. 2002), astrometric calibration (Pier et al. 2002), selection of the galaxy spectroscopic samples (Strauss et al. 2002; Eisenstein et al. 2001), and spectroscopic tiling (Blanton et al. 2002).

The present analysis is based on the Northern stripe, which covers $145^\circ.89 < \alpha < 234^\circ.57$ (excluding three unobserved gap regions; $152^\circ.46 < \alpha < 156^\circ.02$, $167^\circ.03 < \alpha < 171^\circ.88$, $201^\circ.57 < \alpha < 205^\circ.36$) and the Southern stripe, which covers $351^\circ.20 < \alpha < 55^\circ.49$. We form a sub-

sample of galaxies with $14.5 < r^* < 17.6$, after correction for Galactic reddening using the maps of Schlegel, Finkbeiner, & Davis (1998). (The SDSS wavelength band used for galaxy target selection is denoted by r' , but we use r^* to indicate apparent magnitudes using preliminary photometric calibration.) The net sample includes 19710 and 15977 galaxies in the Northern and the Southern stripes, respectively. The resulting apparent-magnitude limited sample has a different mix of galaxy types at different redshifts. We do not consider the effect of this redshift dependence in the following analysis. Note, however, that Hoyle et al. (2002) find a small difference of the two-dimensional genus for the reddest and bluest galaxies.

We estimate the genus for the three-dimensional galaxy distribution in redshift space. For this purpose, we use the comoving distance computed from the observed redshift z (after correction for the Local Group motion) of each galaxy:

$$r(z) = \int_0^z \frac{1}{\sqrt{\Omega_0(1+z')^3 + (1 - \Omega_0 - \lambda_0)(1+z')^2 + \lambda_0}} dz', \quad (1)$$

where Ω_0 is the matter density parameter and λ_0 is the dimensionless cosmological constant. Because of this mapping, the density fields, and thus the genus constructed from the observed galaxy distribution, are dependent on the assumed set of cosmological parameters discussed below.

3. Mock samples from N-body simulations

To quantitatively evaluate various observational effects on the genus statistics such as the shape of survey volume, the redshift distortion effect, and the radial selection function, we generate various different mock samples which are summarized in Table 1. All the mock catalogs are constructed from a series of the P³M N-body simulations by Jing & Suto (1998) which employ 256^3 particles in a $(300h^{-1}\text{Mpc})^3$ periodic comoving box. These simulations use Gaussian initial conditions and the cold dark matter (CDM) transfer function (Bardeen et al. 1986). We neglect the light-cone effect (Hamana, Colombi & Suto 2001) over the survey volume for simplicity, and therefore use the $z = 0$ snapshot simulation data in two cosmological models; Standard CDM (SCDM) with $\Omega_0 = 1$, $\lambda_0 = 0$, $h = 0.5$, $\Gamma = 0.5$, and $\sigma_8 = 0.6$, and Lambda CDM (LCDM) with $\Omega_0 = 0.3$, $\lambda_0 = 0.7$, $h = 0.7$, $\Gamma = 0.21$, and $\sigma_8 = 1.0$, where h is the Hubble constant in units of 100km/s/Mpc, Γ is the shape parameter of the transfer function, and σ_8 is the r.m.s. mass fluctuation amplitude at $8h^{-1}\text{Mpc}$.

To simulate the effect of the shape of the survey volume, we extract “Wedge(r)” samples of dark matter particles from the full simulation cube data in real space so that they have exactly the same volume shape as the Northern and Southern stripe regions. To construct mock samples that extend beyond the simulation box size, we duplicate particles using the periodic boundary condition. The unobserved gap regions are also taken into account. To examine the effect of redshift space distortions, we construct “Wedge(z)” samples similar to

the Wedge(r) samples but in redshift space using the radial peculiar velocity of the simulation particles to perturb the positions along the line of sight.

To include the selection function due to the apparent-magnitude limits, we construct “Wedge(ϕ)” samples from the Wedge(r) samples by applying the radial selection function expected for our limits $14.5 < r^* < 17.6$ and then add the peculiar velocity to each particle, so that the resulting particle distribution matches the redshift distribution of the observed galaxies (see subsection 5.2). Note that this procedure implicitly assumes that the luminosity functions constructed for the observed redshifts of objects do not suffer from the redshift-distortion effect. In order to check this, we also constructed the corresponding “Wedge(ϕ)” samples by directly applying the selection function to the Wedge(z) samples. Reassuringly, the two mock samples constructed from the slightly different procedures turned out to yield almost indistinguishable genus curves. This may be explained by the fact that the luminosity functions are constructed with respect to the mean redshift of objects, and thus the peculiar velocity effect is statistically canceled. Finally, we construct “Wedge($\phi \cdot \phi^{-1}$)” samples that are spatially the same as the Wedge(ϕ) samples, but where each simulation particle is weighted by the inverse of the selection function in the analysis so as to correct for the selection function in a straightforward manner. This yields the same correction to the simulated density field that is applied to the SDSS EDR galaxies when we compute the genus.

Table 1. Mock samples and SDSS EDR data adopted in the present analysis (for $z_{\max} = 0.1$).

Name	volume shape	real/redshift	$\phi(z)$	ϕ^{-1} correction	No. of particles/galaxies
Full simulation	$(300h^{-1}\text{Mpc})^3$ cube	real-space	No	—	256^3
Wedge (r)	wedge($z < z_{\max}$)	real-space	No	—	$\sim 37000(z_{\max} = 0.1)$
Wedge (z)	wedge($z < z_{\max}$)	redshift-space	No	—	$\sim 37000(z_{\max} = 0.1)$
Wedge (ϕ)	wedge($z < z_{\max}$)	redshift-space	Yes	No	$\sim 7500(z_{\max} = 0.1)$
Wedge ($\phi \cdot \phi^{-1}$)	wedge($z < z_{\max}$)	redshift-space	Yes	Yes	$\sim 7500(z_{\max} = 0.1)$
SDSS EDR (North)	wedge($z < z_{\max}$)	redshift-space	Yes	Yes	$7758(z_{\max} = 0.1)$
SDSS EDR (South)	wedge($z < z_{\max}$)	redshift-space	Yes	Yes	$6580(z_{\max} = 0.1)$

4. The Genus Statistic

4.1. Computing the genus

The genus, $G(\nu_\sigma)$, is defined as $-1/2$ times the Euler characteristic of the isodensity contour of the density field δ at the threshold level of ν_σ times the r.m.s. fluctuation σ . In practice this is equal to (number of holes) $-$ (number of isolated regions) of the isodensity surface. In this paper, we use $g(\nu_\sigma)$ to refer to the genus per unit volume, i.e., $g(\nu_\sigma) \equiv G(\nu_\sigma)/V$

where V is the volume of the survey. The genus G of the isodensity contour contained within the survey volume is obtained by integrating the curvature of that surface using the Gauss-Bonnet theorem

$$G = -\frac{1}{4\pi} \int \frac{1}{R_1 R_2} dA \quad (2)$$

where R_1 and R_2 are the principal radii of curvature of the surface. This form of the genus allows for partial contributions to the genus from structures that extend beyond the survey boundaries.

In this paper we primarily examine the genus as a function of the threshold level ν_σ , which indicates that the isodensity surface is drawn at ν_σ times the r.m.s. density fluctuation σ of the density field after smoothing, as described below. Note carefully that the description of the density threshold in terms of ν_σ differs from the definition of ν_f used in some papers on the genus statistics (e.g., Gott et al. 1989), in which ν_f is used to parameterize the fraction f of the volume that lies on the high-density side of the contour,

$$f = \frac{1}{\sqrt{2\pi}} \int_{\nu_f}^{\infty} e^{-x^2/2} dx. \quad (3)$$

We label this volume-fraction definition of the threshold ν_f in the discussion below. In section 6 we present our final results in terms of both ν_σ and ν_f .

For a Gaussian random density field, the genus per unit volume is

$$g_{\text{RG}}(\nu_\sigma) = \frac{1}{(2\pi)^2} \left(\frac{\sigma_1^2}{3\sigma^2} \right)^{3/2} (1 - \nu_\sigma^2) \exp\left(-\frac{\nu_\sigma^2}{2}\right), \quad (4)$$

where $\sigma_1 \equiv \langle |\nabla \delta|^2 \rangle^{1/2}$ and $\sigma \equiv \langle \delta^2 \rangle^{1/2}$. Here $\nabla \delta$ denotes the spatial derivative of the density field δ and $\langle \cdots \rangle$ is the average over the probability distribution function (PDF) of δ and $\nabla \delta$ (c.f., Doroshkevich et al. 1970; Adler 1981; Bardeen et al. 1986; Gott, Mellot & Dickinson 1986; Hamilton et al. 1986).

We compute the genus for density fields from mock samples and SDSS galaxies using the CONTOUR 3D routine (Weinberg 1988). We use the cloud-in-cell (CIC) method to assign survey galaxies and dark matter particles to cells on a 256^3 grid. We Fourier transform the density field, multiply it by the Fourier transform of a Gaussian window with smoothing length R_G , then transform it back to real space. We use the conventional definition of the Gaussian smoothing length R_G for the smoothing kernel

$$W_G(r) = \frac{1}{\sqrt{2\pi} R_G} \exp\left(-\frac{r^2}{2R_G^2}\right). \quad (5)$$

This definition of R_G differs from some previous papers in which the “smoothing length” is defined as $\lambda_G = \sqrt{2} R_G$. The smoothed density fields are used to define the isodensity surfaces with a given threshold ν_σ . The genus is evaluated by integrating the deficit angles (contributions to the curvature at grid cell vertices) over the isodensity surfaces. In the wedge mock samples, integration of the deficit angles is performed only at grid cells located inside the wedge region;

the contribution at grid cells on the boundary and outside the region is neglected. Examples of isodensity surfaces for the different mock samples as well as for the SDSS galaxies are illustrated in Figure 1.

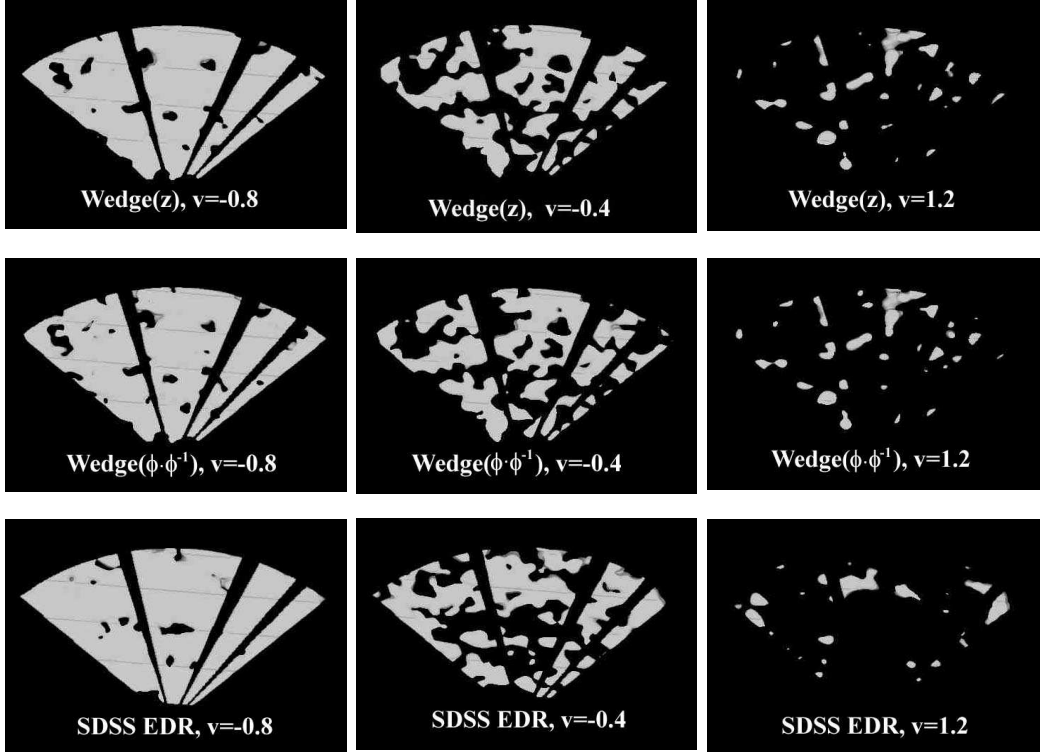


Fig. 1. Isodensity contour surfaces for different simulation mock samples and SDSS EDR galaxies. The Gaussian smoothing length is $R_G = 5h^{-1}\text{Mpc}$. From top to bottom are contours for Wedge(z), Wedge($\phi \cdot \phi^{-1}$), and SDSS EDR galaxies (corrected for the selection function). Left, center and right panels illustrate the isodensity contours corresponding to $\nu_\sigma = -0.8$, -0.4 and 1.2 .

4.2. Log-normal model prediction vs. Full simulation

Since the one-point PDF of dark matter particles in our simulations is well approximated by the log-normal PDF (Kayo et al. 2001), it is natural to expect that the log-normal model can be used to predict the genus. Matsubara & Yokoyama (1996) derived the genus expression assuming that the nonlinear density field of dark matter has a one-to-one mapping to its primordial Gaussian field. If one adopts the log-normal mapping, the result is explicitly written as

$$g_{\text{mass,LN}}(\nu_m) = g_{\text{max,LN}}[1 - x_{\text{LN}}^2(\nu_m)] \exp\left[-\frac{x_{\text{LN}}^2(\nu_m)}{2}\right], \quad (6)$$

$$x_{\text{LN}}(\nu_m) \equiv \frac{\ln[(1 + \nu_m \sigma_{\text{mm}})\sqrt{1 + \sigma_{\text{mm}}^2}]}{\sqrt{\ln(1 + \sigma_{\text{mm}}^2)}}, \quad (7)$$

where $\nu_m = \delta_{\text{mass}}/\sigma_{\text{mm}}$, $\sigma_{\text{mm}} = \langle \delta_{\text{mass}}^2 \rangle^{1/2}$, δ_{mass} is the mass density fluctuation, and the maximum value, $g_{\text{max,LN}}$ is given by:

$$g_{\text{max,LN}} = \frac{1}{(2\pi)^2} \left[\frac{\langle |\nabla \delta_{\text{mass}}|^2 \rangle}{3(1 + \sigma_{\text{mm}}^2) \log(1 + \sigma_{\text{mm}}^2)} \right]^{3/2}. \quad (8)$$

The one-to-one mapping assumption is much stronger than the statement that the one-point PDF is empirically fitted to the log-normal PDF. In particular, the prediction (eq. [6]) accurately describes previous simulation results for dark matter particles (Matsubara & Yokoyama 1996; Hikage, Taruya & Suto 2002).

Figure 2 compares the total genus, $G(\nu_\sigma)$, for the particle distribution in the full $(300h^{-1}\text{Mpc})^3$ cubic volume with the log-normal prediction (eq.[6]). The plotted error bars represent the standard deviation among three different realizations of full simulations. We use Gaussian smoothing lengths $R_G = 3h^{-1}\text{Mpc}$ (Upper-left), $5h^{-1}\text{Mpc}$ (Upper-right), $7h^{-1}\text{Mpc}$ (Lower-left), and $10h^{-1}\text{Mpc}$ (Lower-right). Also shown are the r.m.s. mass fluctuation amplitudes, $\sigma = \sigma(R_G)$ on the Gaussian smoothing scale R_G . The values of σ and the quoted standard deviation for simulations are directly evaluated from the three different realizations, while those for the log-normal model prediction are *not* fitted to the simulation data, but rather are computed using the nonlinear power spectrum of Peacock & Dodds (1996) and the assumed set of cosmological parameters. In this sense, this comparison does not have any free fitting parameters. Figure 2 shows that the log-normal model describes well both the amplitude and the shape of $G(\nu_\sigma)$ for the simulation data at all smoothing lengths.

5. Observational systematic effects on genus statistics evaluated with mock samples

In what follows, we begin with the full simulation particle distribution and consider the key observational effects in a cumulative manner: the survey volume geometry, redshift-space distortion, radial selection function due to the magnitude-limit, and correction for the selection function. These effects are discussed in the following plots and subsections. In this section, we show results of mock samples that mimic the Northern stripe using simulations of the LCDM model.

5.1. Full Simulation vs. Wedge(r): Effect of survey shape

Figure 3 shows the effect of the survey volume shape by comparing the two mock samples, Full and Wedge(r). The volume of Wedge(r) is selected to reproduce the geometry of SDSS EDR North. The mean and standard deviation of the genus are estimated from fifteen independent wedge samples drawn from the three different realizations of the full simulations. To account for the survey geometry, the CONTOUR3D routine uses reference mask particles randomly distributed over the survey region. The density field of mask particles is computed on a grid with the CIC method, then smoothed in the same way as the dark matter particles evolved in

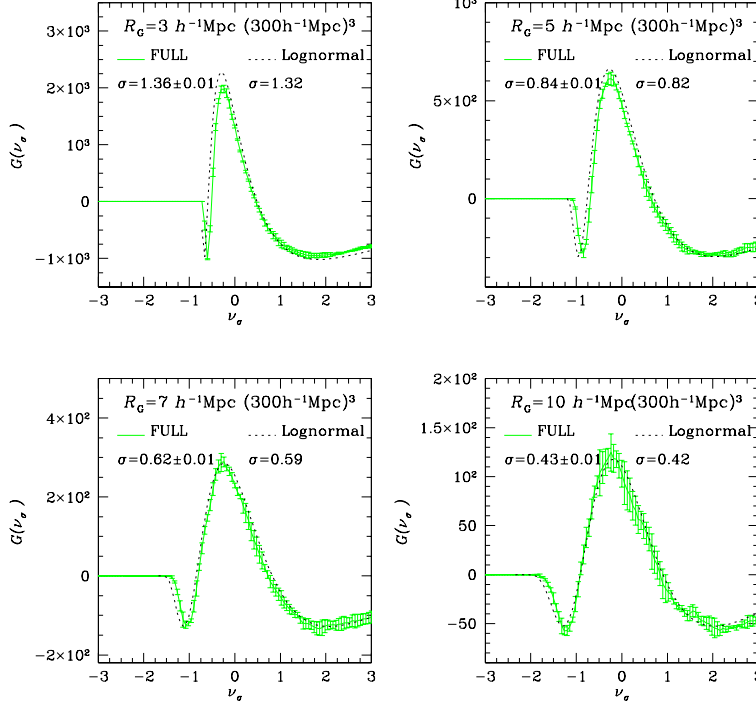


Fig. 2. Genus $G(\nu_\sigma)$ as a function of $\nu_\sigma \equiv \delta/\sigma$ for the particle distribution in the full N-body simulation data (solid lines) compared with the log-normal model predictions (dotted lines) for several Gaussian smoothing lengths R_G . The values of σ in each panel show the rms density fluctuations on the corresponding smoothing scale.

the simulations (e.g., Moore et al. 1992, Melott & Dominik 1993).

In an apparent-magnitude limited galaxy survey, the number density of observed galaxies decreases with redshift. Reliable reconstruction of density fields from the discrete particle distribution requires that the smoothing length R_G approximately exceeds the mean separation length of galaxies at the redshift. (Using too small a smoothing length would result in isodensity contours that are spheres around each particle.) To satisfy this criterion, we set the upper limit of the redshift $z_{\max} = z_{\max}(R_G)$ so that R_G equals the mean separation of the magnitude-limited galaxy sample at z_{\max} (Vogeley et al. 1994). The values of z_{\max} , the resulting numbers of galaxies and the minimum values of the absolute magnitude M_{\min} for SDSS EDR galaxy subsamples that we consider below are listed in Table 2 as a function of R_G . We also list the number of independent resolution elements in each sample,

$$N_{\text{res}} \equiv \frac{V_{\text{survey}}(< z_{\max})}{(2\pi)^{3/2} R_G^3}, \quad (9)$$

which provides an approximate measure of the sample variance in the current analysis, roughly proportional to $N_{\text{res}}^{1/2}$. Gott et al. (1989) noted that $N_{\text{res}} \approx 100$ yields a fractional error of $\sim 25\%$ in estimating the genus curve. Comparison of N_{res} as a function of R_G shows that our results for $R_G = 5h^{-1}\text{Mpc}$ and $R_G = 7h^{-1}\text{Mpc}$ are statistically more reliable than those for the other

two smoothing scales.

Table 2. Samples of SDSS EDR galaxies analyzed for different smoothing lengths R_G assuming LCDM model parameters.

R_G	z_{\max}	Northern stripe			Southern stripe		
		number of galaxies	N_{res}	M_{min}	number of galaxies	N_{res}	M_{min}
3	0.04	1275	94	-21.2	1730	90	-21.1
5	0.10	7758	248	-22.8	6580	236	-22.6
7	0.14	11294	214	-23.1	9050	203	-22.9
10	0.17	12770	132	-23.1	10203	126	-23.2

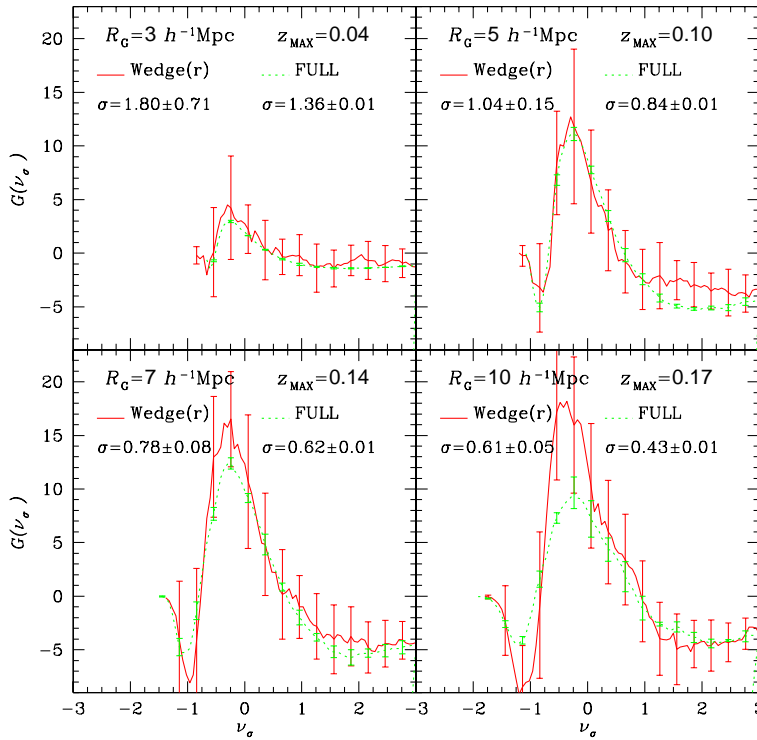


Fig. 3. Effect of the survey volume shape on $G(\nu_\sigma)$ with different R_G . Solid lines show results for the full simulations. Dotted lines show the genus for the Wedge(r) mock samples. The plotted error-bars represent the one standard deviation computed from the 15 independent Wedge(r) mock samples sampled at $\Delta\nu_\sigma = 0.25$. To make this comparison, the genus amplitude of the full simulation is normalized by the ratio of the full and wedge volumes.

To correct for the different volumes of the full and wedge samples, we divide the genus of the full sample by the appropriate volume ratio. Comparison of the genus shows that the Wedge(r) mock samples yield a larger genus amplitude than that of the full simulations, especially for $R_G > 7h^{-1}\text{Mpc}$. Because the thickness of the wedge survey region of SDSS EDR is merely $13h^{-1} \text{Mpc}$ at $z = 0.1$, a large fraction of the smoothing region lies outside the

survey boundary, which leads to the unphysical behavior revealed here. In other words, our 3D analysis essentially reduces to a 2D analysis for $R_G > 7h^{-1}\text{Mpc}$. Some of the clustering signal is effectively smoothed to beyond the survey boundary and not taken into account in the analysis which only includes grid vertices within the survey volume. Thus the signal-to-noise ratio for structure within the survey is somewhat reduced. Therefore it may not be meaningful to attempt to understand the detailed behavior of the genus curve on these larger smoothing scales for such a geometry. Nevertheless one can still explore the cosmological implications by comparing the results between the (final) mock samples and the observed galaxies, since both data and simulations are treated in the same fashion.

5.2. *Wedge(z) vs. Wedge($\phi \cdot \phi^{-1}$): radial selection effect*

The Wedge(z) samples differ from the Wedge(r) samples only by introduction of the distortion of redshift space caused by peculiar velocities. This distortion has minimal effect on the genus, consistent with previous results (Matsubara 1996; Matsubara & Suto 1996). Thus, the more important observational effect comes from the apparent-magnitude limit of the sample, which changes the mean galaxy number density with redshift. Appropriate correction for this selection function is necessary to accurately define the isodensity surfaces in apparent-magnitude limited samples.

We compute the selection function, $\phi(z)$, by integrating over the Schechter form of the luminosity function,

$$\phi(z) \propto \int_{M_{\min}(z)}^{M_{\max}(z)} \phi_* [10^{0.4(M_* - M)}]^{\alpha+1} \exp[-10^{0.4(M_* - M)}] dM, \quad (10)$$

with parameters measured in the r' band by Blanton et al. (2001) for the SDSS, $M_* - 5\log_{10} h = -20.83(-20.67)$, $\alpha = -1.20(-1.15)$, $\phi_* = 1.46(1.87) \times 10^{-2} h^3 \text{Mpc}^{-3}$ for analyses that assume the cosmological parameters of the LCDM (SCDM) cosmological model. The limits of integration are the absolute magnitude limits

$$M_{\max/\min}(z) = m_{\max/\min} - 5\log[(1+z)r(z_{\max/\min})/10\text{pc}] - K(z). \quad (11)$$

We use apparent-magnitude limits $m_{\max} = 17.6$, $m_{\min} = 14.5$, following Blanton et al. (2001), and apply an approximate K-correction factor $K(z) = 0.9z$ valid for the typical galaxy color of $g^* - r^* = 0.65$ (Fukugita et al. 1995). Figure 4 shows the number density distribution of SDSS EDR galaxies (histogram) compared with fits from equation (10) for the cosmological parameters of both the LCDM and SCDM models.

We randomly select dark matter particles in the Wedge(z) sample according to the above selection function to reproduce the number of observed SDSS galaxies in the current sample. Then we attempt to correct for the selection effect simply by weighting each particle by the inverse of the selection function $\phi(z)^{-1}$ (e.g., Rhoads et al. 1994; Vogeley et al. 1994) before smoothing the density field. The contours shown in Figure 1 adopt this correction, which illustrates that this correction accurately reproduces the structure. Figure 5 shows more

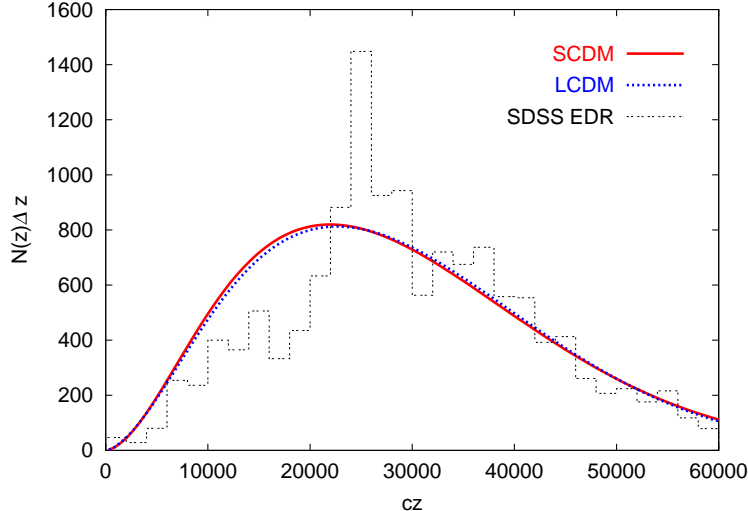


Fig. 4. Number density distribution of SDSS EDR galaxies. The redshift width Δz of the histogram is 1/150. Fits from equation (10) are plotted assuming the cosmological parameters of the LCDM (solid line) and SCDM (dotted line) models.

quantitatively that the correction is very accurate for the genus statistics. Therefore we compare the genus of the SDSS galaxies and the mock samples after applying the $1/\phi(z)$ correction to their redshift-space distributions.

6. Genus of the SDSS EDR Sample

Finally, we present the genus estimated for the apparent-magnitude limited SDSS EDR galaxy samples. The galaxy density fields are corrected for the selection function as discussed above. Figures 6 and 7 show the genus curves (*filled circles*) for the SDSS galaxies assuming the cosmological parameters of the LCDM and SCDM models, respectively, and the genus of the corresponding mock samples.

The plotted error-bars for each model prediction represent the 1 standard deviation computed from 15 independent mock samples. To within these uncertainties, we conclude that the genus for the SDSS EDR galaxies is consistent with the LCDM model prediction, but does not agree with that of SCDM.

Galaxy biasing is another source of uncertainty for relating the observed genus curves to those obtained from the mock samples generated from the distribution of dark matter particles (e.g., Colley et al. 2000; Hikage, Taruya, Suto 2001). If LCDM is the correct cosmological model, then the good match of the genus for mock samples from the LCDM simulations to the observed SDSS genus may indicate that nonlinearity in the galaxy biasing is relatively small, at least small enough that it does not impact the genus statistic. In separate work, Kayo et al. (2002) showed that the biasing parameter for the SDSS EDR galaxies is close to unity and that this biasing is approximately scale-independent if LCDM is assumed. This linear biasing

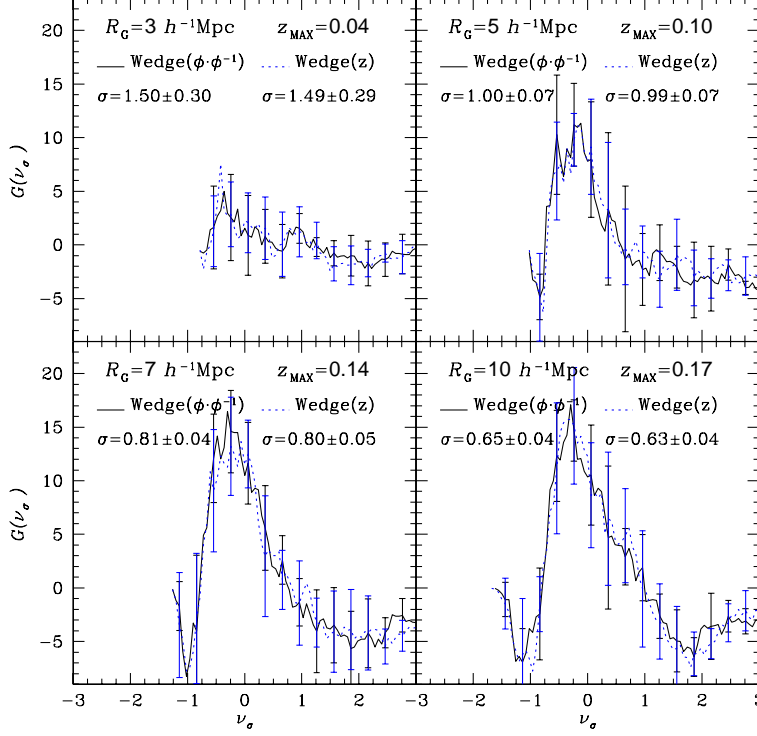


Fig. 5. Genus, $G(\nu_\sigma)$, for Wedge(z) (solid lines) and Wedge($\phi \cdot \phi^{-1}$) mock samples, for different smoothing lengths R_G . This comparison shows that weighting galaxies in an apparent-magnitude limited sample by the inverse of the selection function provides a correct estimate of the genus.

does not affect the genus curve, thus our conclusion remains unchanged.

Differences between the genus curves for the mock samples drawn from simulations of the LCDM and SCDM models arise largely from the power spectra for those models which affect only the amplitude of the genus curve (see eqs.[4] and [6] – [8]). The shapes of the genus curves for the two models are almost identical. In other words, the present genus analysis places constraints on the cosmological models that are consistent with previous results using the 2PCF, but it does not yet exploit the full advantage of the genus statistics as a complementary statistic to the conventional 2PCF. Nevertheless, it is encouraging that one can draw meaningful cosmological conclusions from the genus analysis on the basis of the available EDR sample from the genus amplitude alone.

Thus far in this paper we have plotted the genus curve as a function of the density threshold parametrized by the number ν_σ of standard deviations above the mean of the smoothed density field. In contrast, the genus is often plotted as a function of the threshold ν_f which is defined so that the volume fraction on the high-density side of the isodensity surface is identical to the volume in regions with density contrast $\delta = \nu_f \sigma$, for a Gaussian random field with r.m.s. density fluctuations σ (see Equation 3). If the evolved density field has a one-to-one correspondence with the initial random-Gaussian field, then this transformation removes the effect of evolution of the PDF of the density field (see section 4.2). Under this assumption, the

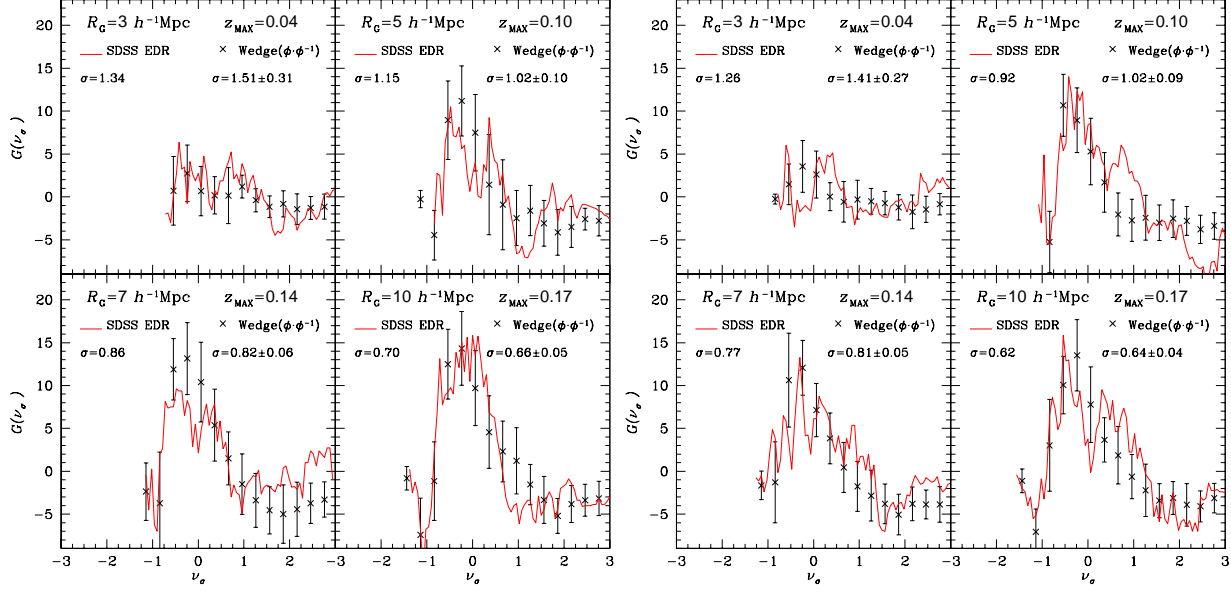


Fig. 6. Comparison of the genus $G(\nu_\sigma)$ for SDSS EDR galaxies with $\text{Wedge}(\phi \cdot \phi^{-1})$ mock samples from LCDM simulations. Plotted separately are the genus curves for the Northern stripe (*Left*) and Southern stripe (*Right*) of the SDSS EDR sample. Error bars are shown for the LCDM prediction

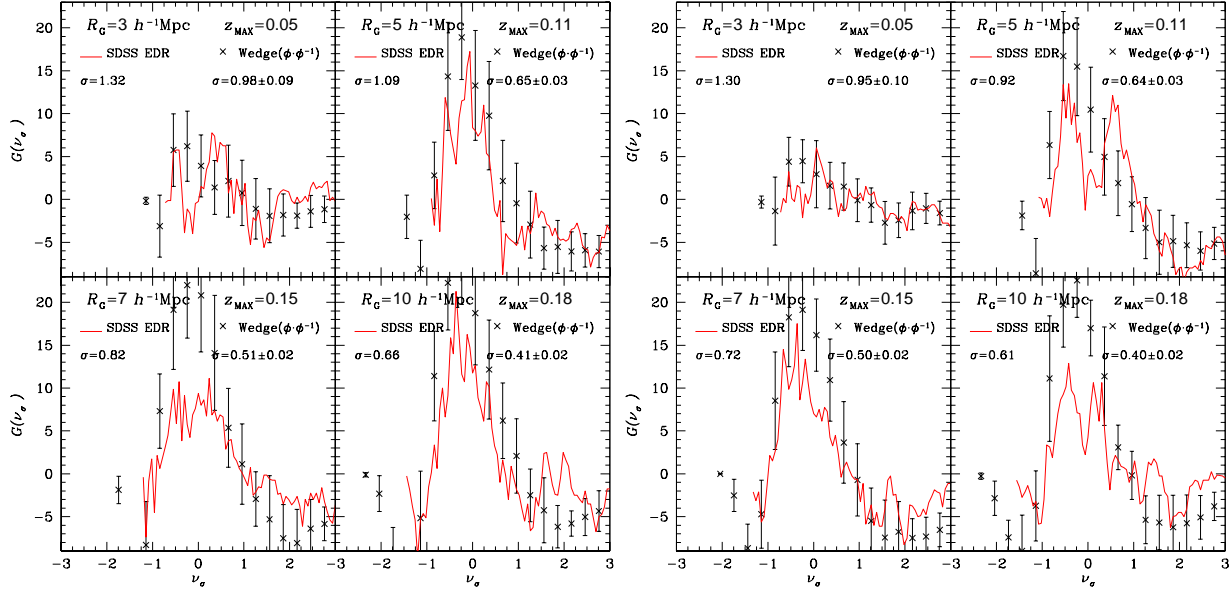


Fig. 7. Same as Figure 6 but in the SCDM model.

genus as a function of volume fraction, expressed as $G(\nu_f)$, is sensitive only to the topology of the isodensity contours rather than evolution with time of the density threshold assigned to a contour. Limitations of the approximation of monotonicity in the relation between initial and evolved density fields are examined by Kayo et al. (2001).

To allow clear comparison with other genus estimates in the literature, in Figures 8 and 9 we replot Figures 6 and 7, respectively, using ν_f . The solid lines indicate the results from the SDSS EDR samples, and the dotted curves show the Gaussian prediction (eq.[4]) with its one free parameter, the amplitude, set by minimizing χ^2 between the SDSS genus and the theoretical curve. The mock sample data are shown as symbols with error bars to indicate the expected sample-to-sample variation for the current data size. Shown in this way, the genus curves for both the data and mock samples appear to agree with the random-Gaussian curve, which may be interpreted to imply that the primordial Gaussianity is confirmed.

A more correct interpretation is that, given the size of the estimated uncertainties, these data do not provide evidence for initial non-Gaussianity, i.e., the data are *consistent* with primordial Gaussianity. In order to go further and place more quantitative constraints on primordial Gaussianity with up-coming data, one needs a more precise and reliable theoretical model for the genus which properly describes the nonlinear gravitational effect possibly as well as galaxy biasing beyond the simple mapping on the basis of the volume fraction (see also Fig. 10 below). A perturbative approach by Matsubara (1994) combined with the extensive simulation mock sample analysis may be a promising strategy for this purpose.

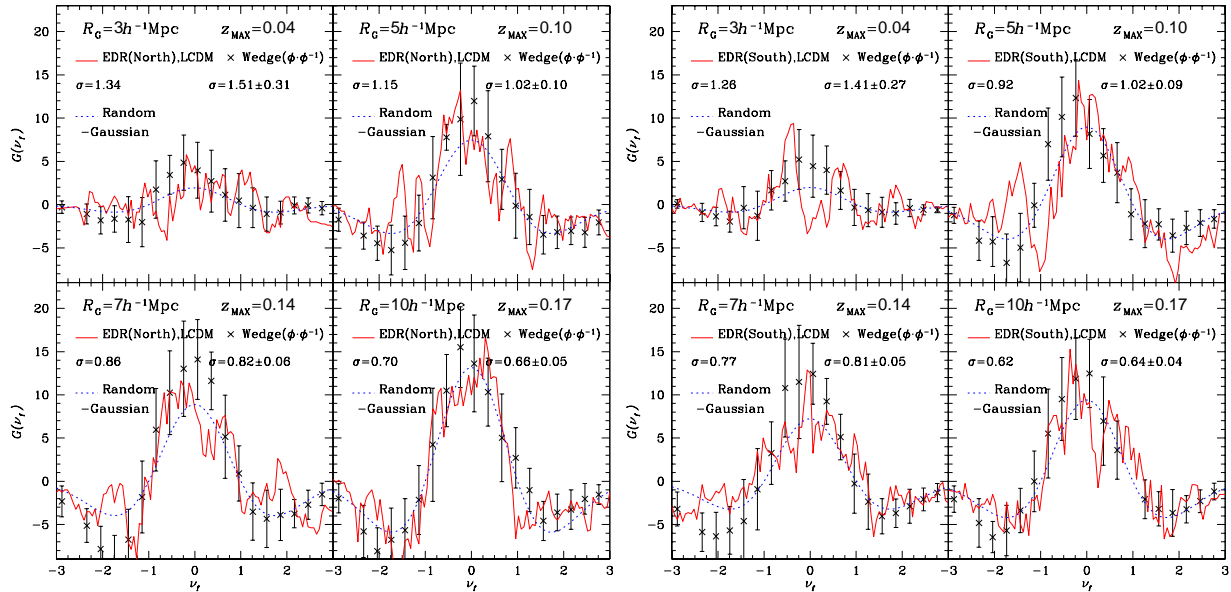


Fig. 8. Same as Figure 6 but plotted as a function of ν_f , the threshold defined through the volume fraction.

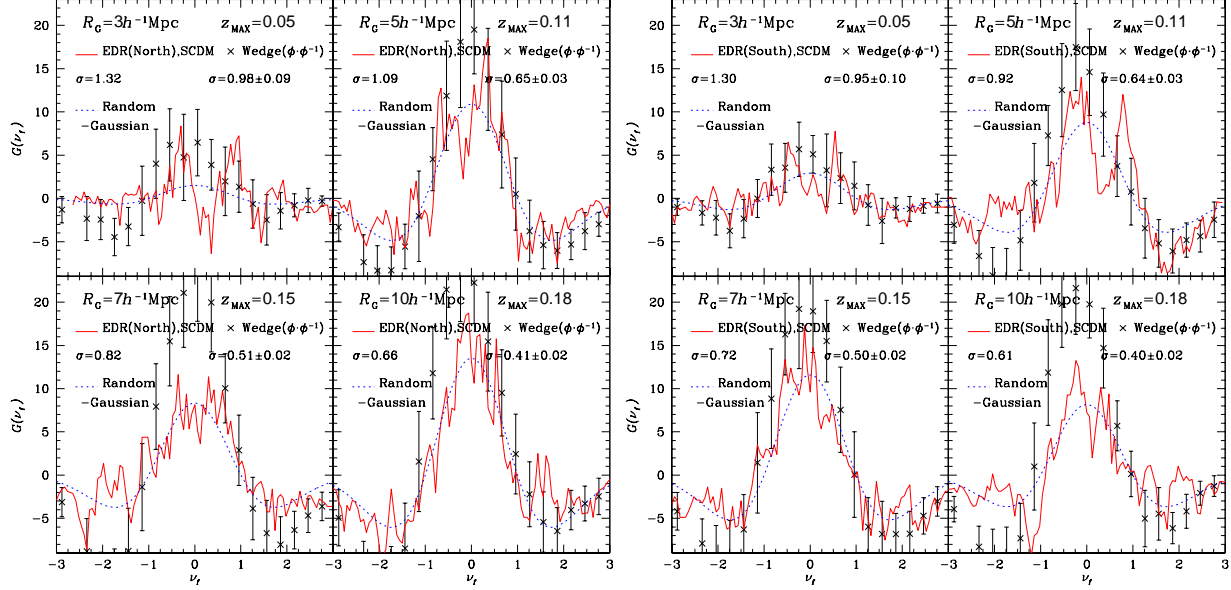


Fig. 9. Same as Figure 8 but in SCDM model.

7. Summary and Conclusions

We present the first analysis of the three-dimensional genus statistics for SDSS EDR galaxy data. Due to the complicated survey volume and the selection function of the current sample, analytic predictions of the corresponding genus statistics are not feasible and we construct extensive mock catalogs from N-body simulations in order to explore the cosmological implications. We also use these mock catalogs to examine the effects of several possible observational systematics on the genus statistic. We find that redshift-space distortions cause minimal changes in the genus curve. However, the slice-like geometry of the SDSS EDR galaxy samples causes large distortions of the genus curve on smoothing scales $R_G > 7h^{-1}\text{Mpc}$. We demonstrate that weighting by the inverse of the selection function with distance in apparent-magnitude limited samples allows recovery of the genus curve. Because the mock catalogs include all of these effects, comparison with theoretical models is possible.

We conclude that the observed shape and amplitude of the genus for the SDSS EDR galaxy sample are consistent with the distribution of dark matter particles in simulations of the LCDM model. In contrast, the SCDM model predictions do not match the amplitude of the observed genus. Comparison of the observed genus curves with the theoretical prediction for a Gaussian random field shows that, within the uncertainties as estimated from the mock samples, the data are consistent with Gaussianity of the primordial density field.

A question for the future is the degree of improvement that one can expect for the larger samples of the SDSS galaxy redshift survey. To predict this, we generate larger mock catalogs by increasing the sky coverage by three times ($\sim 7 \times 10^4$ galaxies) and thirty times ($\sim 7 \times 10^5$ galaxies) relative to the Northern stripe in EDR. Figure 10 shows the predicted genus in LCDM

and SCDM models (see also Colley et al. 2000 for predictions of genus results for the SDSS). The positions of the symbols in those panels correspond to the data of one specific mock sample, but with error-bars estimated from the 15 independent mock samples. For reference, the lines in upper panels show the mean genus curves averaged over the 15 independent mock samples, while the lines in lower panels indicate the fit of the random-Gaussian prediction to the plotted sample data. Of interest is that the smaller uncertainties in this future sample will put much stronger constraints on cosmological models, the nonlinear nature of the galaxy biasing, and primordial Gaussianity than those presented here.

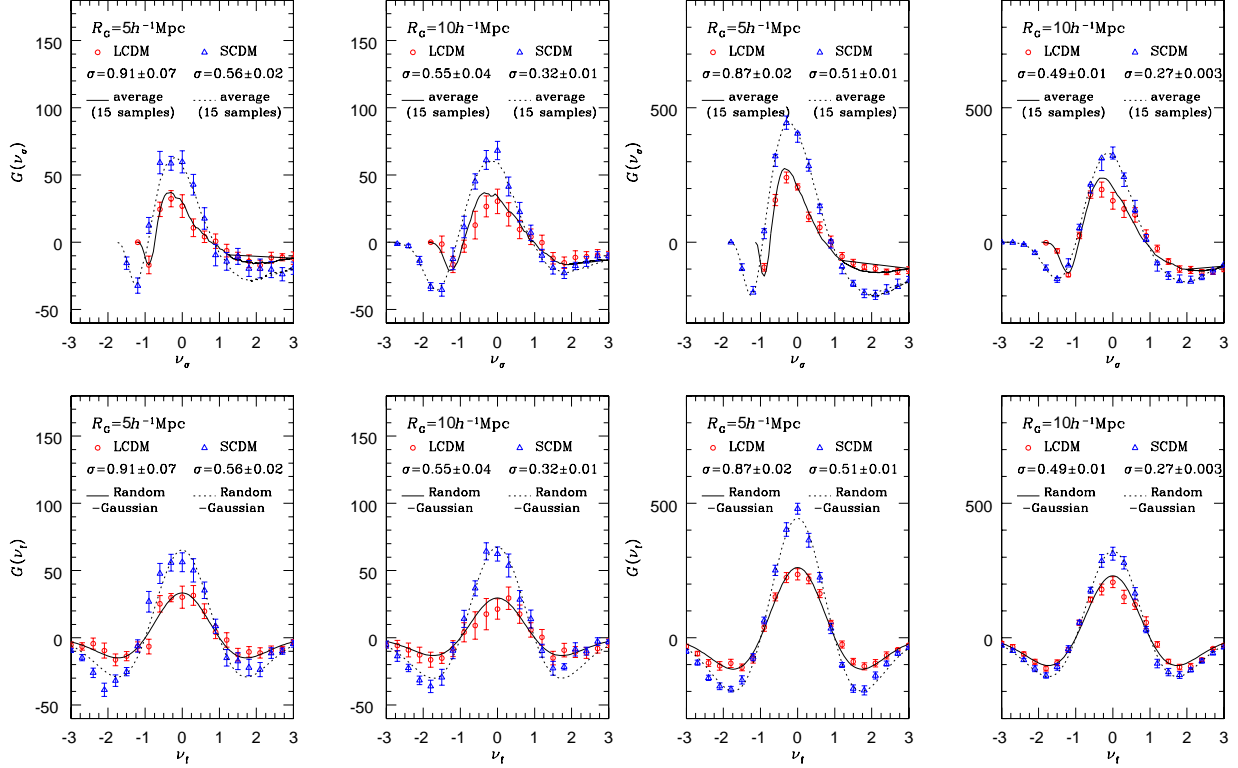


Fig. 10. Prediction of the genus for future samples of SDSS galaxies, using mock catalogs in LCDM (*Open circles and Solid lines*) and SCDM (*Open triangles and Dotted lines*) From left to right, $R_G = 5h^{-1}\text{Mpc}$ with 7×10^4 galaxies, $R_G = 10h^{-1}\text{Mpc}$ with 7×10^4 galaxies, $R_G = 5h^{-1}\text{Mpc}$ with 7×10^5 galaxies, and $R_G = 10h^{-1}\text{Mpc}$ with 7×10^5 galaxies. Upper and lower panels plot the total number of genus in terms of ν_σ and ν_t , respectively.

We thank Y. P. Jing for kindly providing us his N-body simulation data which were used in generating mock samples. I. K. gratefully acknowledges support from the Takenaka-Ikueikai fellowship. Numerical computations were carried out at ADAC (the Astronomical Data Analysis Center) of the National Astronomical Observatory, Japan. This research was supported in part by the Grant-in-Aid from Monbu-Kagakusho and Japan Society of Promotion of Science (12640231, 13740150, 14102004, and 1470157). MSV and FH acknowledge support

from NSF grant AST-0071201 and a grant from the John Templeton Foundation. JRG acknowledges support from NSF grant AST-9900772.

Funding for the creation and distribution of the SDSS Archive has been provided by the Alfred P. Sloan Foundation, the Participating Institutions, the National Aeronautics and Space Administration, the National Science Foundation, the U.S. Department of Energy, the Japanese Monbu-Kagakusho, and the Max Planck Society. The SDSS Web site is <http://www.sdss.org/>.

The SDSS is managed by the Astrophysical Research Consortium (ARC) for the Participating Institutions, which are the University of Chicago, Fermilab, the Institute for Advanced Study, the Japan Participation Group, the Johns Hopkins University, Los Alamos National Laboratory, the Max-Planck-Institute for Astronomy (MPIA), the Max-Planck-Institute for Astrophysics (MPA), New Mexico State University, Princeton University, the United States Naval Observatory, and the University of Washington.

References

- Adler, R.J. 1981, *The Geometry of Random Fields* (Chichester: Wiley)
- Bardeen, J. M., Bond, J. R., Kaiser, N., & Szalay, A. S. 1986, ApJ, 304, 15
- Barrow, J.D., Bhavsar, S.P., & Sonoda, D.H. 1985, MNRAS 216, 17
- Blanton, M. R. et al. 2001, AJ, 121, 2358.
- Blanton, M. R., Lupton, R.H., Maley, F.M., Young, N., Zehavi, I., & Loveday, J. 2002, AJ submitted.
- Canavezes, A., et al., 1998, MNRAS, 297, 777
- Coles, P., & Jones, B. 1991, MNRAS, 248, 1
- Coles, P., & Plionis, M., 1991, MNRAS, 250, 75
- Colley, W.N., Gott III, J.R., Weinberg, D.H., Park, C., & Berlind, A.A. 2000, ApJ, 529, 795
- Dodelson, S., et al. 2002, ApJ submitted, astro-ph/0107421
- Doroshkevich, A. G. 1970, Astrofizika, 6, 581 (English transl. Astrophysics, 6, 320)
- Eisenstein, D. J. et al. 2001, AJ, 122, 2267
- Fukugita, M., Shimasaku, K., & Ichikawa, T. 1995, PASP, 107, 945
- Fukugita, M., Ichikawa, T., Gunn, J.E., Doi, M., Shimasaku, K., & Schneider, D. P. 1996, AJ. 111, 1748
- Gott, J. R., Mellot, A. L., & Dickinson, M. 1986, ApJ, 306, 341
- Gott, J. R. et al. 1989, ApJ, 340, 625
- Gunn, J. et al. 1998, ApJ, 116, 3040
- Hamana, T., Colombi, S., & Suto, Y. 2001, A&A, 367, 18
- Hamilton, A. J. S., Gott, J. R., & Weinberg, D. 1986, ApJ, 309, 1
- Hamilton, A. J. S., Matthews, A., Kumar, P., & Lu, E. 1991, ApJL, 374, L1.
- Hikage, C., Taruya, A., & Suto, Y. 2001, ApJ, 556, 641
- Hikage, C., Taruya, A., & Suto, Y. 2002, PASJ, submitted
- Hogg, D.W., Finkbeiner, D.P., Schlegel, D.J., & Gunn, J.E. 2001, AJ, 122, 2129
- Hoyle, F., Vogeley, M.S. & Gott, J. R. III, 2002a, ApJ, 570, 44
- Hoyle, F., Vogeley, M.S., Gott, J.R. III, Blanton, M., Tegmark, M., Weinberg, D.H, Bahcall, N., Brinkmann, J., & York, D.G 2002b, ApJ, submitted, astro-ph/0206146
- Infante, L. et al. 2002, ApJ, 567, 1551
- Jing, Y. P., & Suto, Y. 1998, ApJ, 494, L5
- Kayo, I., Taruya, A., & Suto, Y. 2001, ApJ, 561, 22
- Kayo, I. et al. 2002, ApJ, submitted
- Lupton, R. H., 2002, in preparation
- Matsubara, T. 1994, ApJL, 434, 43
- Matsubara, T. 1996, ApJ, 457, 13.
- Matsubara, T., & Suto, Y. 1996, ApJ, 460, 51
- Matsubara, T., & Yokoyama, J. 1996, ApJ, 463, 409
- Mecke, K.R., Buchert, T. & Wagner, H. 1994, A&A, 288, 697
- Melott, A. L., 1987, Topology of the Universe: Motivation for the Study of Large -Scale Structure, in Proceedings of the XIIIth Texas Symposium on Relativistic Astrophysics, M. Elmer ed, 1987, World Scientific Publishing

- Melott, A. L., & Dominik, K. 1993, ApJS, 86, 1
- Moore, B., Frenk, C.S., Weinberg, D. H., Saunder, W., Lawrence, A., Ellis, R.S., Kaiser, N., Efstathiou, G., & Rowan-Robinson, M. 1992, MNRAS, 256, 477
- Park, C., Gott, J. R. III, & Choi, Y. J. 2001, ApJ, 553, 33
- Park, C., Gott, J. R. III, da Costa, L. N., 1992, ApJ, 392, L51
- Park, C., Gott, J. R. III, Melott, A. L., & Karachentsev, I. D., 1992, ApJ, 387, 1
- Peacock, J.A., & Dodds, S.J. 1996, MNRAS, 280, L19
- Peebles, P. J. E. 1980, The Large-Scale Structure of the Universe (Princeton: Princeton University Press)
- Pier, J., et al. 2002, AJ submitted
- Plionis, M., Valdarnini, R. & Coles, P., 1992, MNRAS, 258, 114
- Rhoads, J.E.R., Gott III, J.R., & Postman, M. 1994, ApJ, 421,
- Schmalzing, J. & T. Buchert, T. 1997, ApJ, 482, L1
- Shandarin, S.F. 1983, Sov.Astron.Lett. 9, 104
- Schechter, P. 1976, ApJ, 203, 297
- Schlegel, D.J., Finkbeiner, D.P., & Davis, M. 1998, ApJ, 500, 525
- Smith, J.A., et al. 2002, AJ, 123, 2121.
- Stoughton, C. et al. 2002, AJ, 123, 485
- Strauss, M.A., et al. 2002 ApJ, in press
- Szalay, A. S., et al. 2002, ApJ submitted, astro-ph/0107419
- Szapudi, I., et al. 2002, ApJ submitted, astro-ph/0111058
- Tegmark, M., et al. 2002, ApJ, 571, 191
- Totsuji, H., & Kihara, T. 1969, PASJ, 21, 221
- Vogeley, M.S., Park, C., Geller, M.J., Huchra, J.P., & Gott III, J.R. 1994, ApJ, 420, 525
- Weinberg, D.H. 1988, PASP, 100, 1373
- White, S.D.M. 1979, MNRAS, 186, 145
- Yoshikawa, K., Taruya, A., Jing, Y.P., & Suto, Y. 2001, ApJ, 558, 520
- York, D. G. et al. 2000, AJ, 120, 1579.
- Zehavi, I., et al. 2002, ApJ, 571, 172